Divalent Metal Ions and the Internal Equilibrium of the Hammerhead Ribozyme†

David M. Long, Frederick J. LaRiviere, and Olke C. Uhlenbeck*

Department of Chemistry and Biochemistry, University of Colorado, Boulder, Colorado 80309-0215

Received July 10, 1995; Revised Manuscript Received September 5, 1995⊗

ABSTRACT: Thermodynamics of RNA cleavage/ligation were measured for a self-cleaving hammerhead ribozyme in the presence of Ca^{2+}, Co^{2+}, Mg^{2+}, and Mn^{2+}. The internal equilibrium, the ratio of cleaved to ligated RNA, decreases with increasing concentrations of each of the four divalent metal ions in a hyperbolic dependence that shows saturation. The metal ion dependence is not due to changes in ionic strength, and the value of the equilibrium constant at saturation is different for each metal ion. The concentration required to achieve half-saturation of the equilibrium is also different for each metal ion, and the order of apparent metal ion dissociation constants correlates with those measured for dissociation of the same metal ions complexed with tRNA and nucleotides. We interpret the divalent metal ion dependence of the equilibrium in terms of a thermodynamic model invoking noncooperative metal ion dissociation from the cleaved RNA. Thus, at 10 mM Mg^{2+}, a commonly employed condition for hammerhead kinetic studies, metal ion dissociation contributes substantially to the free energy of the equilibrium and drives the hammerhead reaction toward cleaved RNA. Temperature dependencies of the equilibrium reveal that while the entropy and enthalpy changes of the equilibrium depend on the identity of the divalent metal ion, in each case a large entropic driving force overcomes an unfavorable change in enthalpy. This agrees with thermodynamics previously measured for an intermolecular hammerhead in the presence of Mg^{2+} [Hertel, K. J., & Uhlenbeck, O. C. (1995) *Biochemistry 34*, 1744−1749].

The hammerhead RNA is a self-cleaving motif found within some plant viroid and virusoid RNAs (Symons, 1992; Long & Uhlenbeck, 1993). The discovery that the hammerhead can be assembled from two separate RNA molecules has facilitated characterization of the site-specific transesterification reaction this RNA catalyzes (Uhlenbeck, 1987; Haseloff & Gerlach, 1988). Development of a kinetic framework for the hammerhead has led to identification and isolation of the chemical cleavage event, which requires divalent metal ions (Prody et al., 1986; Dahm & Uhlenbeck, 1991; Fedor & Uhlenbeck, 1992; Hertel et al., 1994). Kinetic studies of hammerhead chemistry using mutant and modified RNAs under different reaction conditions have provided the basis for our understanding of hammerhead structure and mechanism (Fedor & Uhlenbeck, 1990; Slim & Gait, 1991; Williams et al., 1992).

In addition to kinetic analyses, thermodynamic studies have recently been used to infer mechanistic aspects of hammerhead chemistry (Hertel et al., 1994; Hertel & Uhlenbeck, 1995). These thermodynamic studies have entailed measuring the "internal equilibrium" of the hammerhead, which is the interconversion of enzyme-bound substrate (ES) with enzyme-bound product (EP). The internal equilibrium constant, defined as $K_{eq}^{int} = EP/ES$, is measured by using a ribozyme RNA that binds substrate and product RNAs through a sufficient number of base pairs to ensure that ES and EP do not dissociate under a wide range of experimental conditions. Measuring K_{eq}^{int} in an intermolecular context revealed that EP is favored over ES by a free energy of 2.9 kcal/mol at 298 K, pH 7.5, and 10 mM Mg^{2+}. Although K_{eq}^{int} does not depend on pH to a significant extent, both temperature and magnesium ion concentration have substantial effects.

The temperature dependence of K_{eq}^{int} shows that the reaction has an unfavorable enthalpy change of about 10 kcal/mol which is overcome by a favorable entropy change of about 40 entropy units. Thus, the cleaved hammerhead is energetically favored over the uncleaved hammerhead for entropic reasons. An important goal is to understand the physical reasons for the entropy and enthalpy observed in the hammerhead internal equilibrium. The enthalpy of the equilibrium has been rationalized by comparing it with enthalpies measured for other RNA transesterification reactions (Hertel & Uhlenbeck, 1995). The hammerhead entropy, however, cannot be compared with entropies of other RNA transesterifications because these are cleavage reactions that have large entropies due to generation of two freely diffusable molecules from a single reactant. In the case of the hammerhead internal equilibrium, the two transesterification products remain bound to the ribozyme after cleavage.

The Mg^{2+} concentration dependence of the internal equilibrium reveals that this ion changes the relative thermodynamic stability of the cleaved and uncleaved forms of the hammerhead (Hertel & Uhlenbeck, 1995). At high magnesium concentrations, K_{eq}^{int} is "saturated" at a value that corresponds to a residual free energy of 1.9 kcal/mol. Thus, the free energy of the internal equilibrium arises from a combination of at least two different effects, one which depends on Mg^{2+} concentration and the other which does not. By establishing physical bases for these effects, we hope to improve our understanding of hammerhead chemistry.

The fraction of free energy independent of Mg^{2+} concentration may result from changes in hammerhead structure or dynamics upon cleavage, and the fraction that depends on Mg^{2+} concentration may be associated with changes in Mg^{2+} binding to the RNA upon cleavage. Hertel and Uhlenbeck (1995) interpreted the Mg^{2+} concentration dependence of the

† This work was supported by NIH Grant GM36944 to O.C.U. and by Postdoctoral Fellowship NIH GM14471 to D.M.L.

* Corresponding author.

⊗ Abstract published in *Advance ACS Abstracts,* October 15, 1995.

0006-2960/95/0434-14435$09.00/0

internal equilibrium in terms of changes in Mg^{2+} binding, but did not ascertain if these changes were increases or decreases in stoichiometry or affinity. This paper addresses this point in more detail. Because the internal equilibrium is dependent on Mg^{2+} ion concentration, we have attempted to correlate aspects of metal ion/RNA binding to effects metal ions have on the internal equilibrium. In this paper, we report the internal equilibrium of the hammerhead in the presence of different divalent metal ions. Instead of the intermolecular HH16 used by Hertel and Uhlenbeck (1995), we have used an intramolecular hammerhead and procedures that simplify measurement of the internal equilibrium.

MATERIALS AND METHODS

RNA Synthesis and Purification. The oligonucleotide P2 was chemically synthesized as previously described (Hertel et al., 1994). 5′-HH2 (Figure 1) was synthesized by run-off transcription from *Bam*HI-linearized plasmid pDL15 using T7 RNA polymerase (Milligan & Uhlenbeck, 1989). Internally ^{32}P-labeled 5′-HH2 (specific activity approximately 3000 Ci/mmol) was obtained using [α-^{32}P]CTP in transcription reactions. After purification by electrophoresis, RNAs were precipitated with ethanol and stored at −20 °C in water. RNA concentrations were measured by assuming a residue extinction coefficient at 260 nm of 8.5×10^3 M^{-1} cm^{-1}.

Thermodynamic Measurements. The temperature dependence of the internal equilibrium for HH2 was measured by combining 2 nM ^{32}P-labeled 5′-HH2 and 1 μM P2 in 100 mM PIPES, pH 6.5, in a final volume of 50 μL. This P2 concentration was sufficient to saturate 5′-HH2 since the K_d for P2 is 0.05 nM at 25 °C and 10 mM Mg^{2+} (Hertel et al., 1994). Under all conditions reported in this study, saturation of 5′-HH2 with P2 was confirmed by showing that higher P2 concentrations had no effect on the internal equilibrium. The solution was heated to 95 °C for 1 min, allowed to cool to room temperature, and mixed thoroughly with 50 μL of a solution containing 20 mM metal chloride and 100 mM PIPES, pH 6.5. By buffering the metal ion solution with 100 mM PIPES, changes in pH due to the acidic metal ions were minimized. Ten microliter aliquots of the resulting solution were transferred to siliconized Eppendorf tubes, layered with 15 μL of mineral oil, and incubated at temperatures ranging from 4 to 37 °C for between 12 and 20 h. These incubation times were shown in separate experiments to be sufficient for equilibrium to be reached. Preliminary experiments showed that siliconized Eppendorf tubes were needed to prevent the RNA from sticking to the tube. This protocol was altered slightly for reactions with Ca^{2+}. It was found that the layering of mineral oil over the Ca^{2+} samples resulted in irreproducible extents of ligation. This artifact was corrected for by omitting the mineral oil, increasing the aliquot volume by 5-fold, and incubating samples at the different temperatures for between 1 and 4 days, all resulting in reproducible data. Reactions with Mg^{2+}, Mn^{2+}, and Co^{2+} were quenched by the addition of 50 μL of 95% formamide, 50 mM EDTA, 0.02% bromophenol blue, and 0.02% xylene cyanol preheated to 100 °C. Reactions with Ca^{2+} were quenched by lowering the pH of the reaction sufficiently to stop catalysis with the addition of 100 μL of 100 mM sodium citrate, pH 3.5, 50 mM EDTA, 6 M urea, 0.02% bromophenol blue, and 0.02% xylene cyanol. Samples were then neutralized with 15 μL of 1 N NaOH. Immediately after quenching, samples were vortexed briefly and stored on ice. These quenching protocols were determined by preliminary experiments necessary to stop the HH2 reaction and give reproducible results. The reactions with Ca^{2+} were more reproducible when using the acid quenching procedure. The ligated and cleaved RNAs were separated on 10% denaturing PAGE, and the ratio of ligated RNA to cleaved RNA was quantitated using a Molecular Dynamics phosphorimager.

The metal ion concentration dependencies of the internal equilibrium were measured by serial dilution of samples containing all reaction components into solutions containing all reaction components except metal ions. Five microliters of solution A, which contained 1 nM ^{32}P-labeled 5′-HH2, 500 nM P2, 100 mM PIPES, pH 6.5, and metal chloride (200 or 150 mM for $MgCl_2$; 100 or 75 mM for $CoCl_2$ and $MnCl_2$), was mixed with 5 μL of solution B, which contained the same components and concentrations as solution A with the exception of no added metal ions. After thorough mixing, 5 μL of this mixture was rediluted in 5 μL of solution B, and the procedure was repeated, yielding a series of samples that differed only in metal ion concentration, each by a factor of 2. The samples were covered with 15 μL of mineral oil in siliconized Eppendorf tubes and incubated at 25 °C for 12−20 h for reactions with Mg^{2+} and for 30−60 min with Mn^{2+} and Co^{2+}. Preliminary experiments showed these times were sufficient for equilibrium to be reached at all the metal ion concentrations. This protocol was altered slightly for reactions with Ca^{2+}. The starting concentrations used were 120 and 80 mM $CaCl_2$, the solution volumes were increased 10-fold, the mineral oil was omitted, and the samples were incubated at 25 °C for 24−30 h. Quench procedures, analysis, and quantitation were the same as described above for the temperature dependence, except 100 μL of formamide quench buffer was used for reactions with Mg^{2+}, Mn^{2+}, and Co^{2+}.

RESULTS

The hammerhead internal equilibrium was studied using an intramolecular configuration (HH2) described previously (Long & Uhlenbeck, 1994) (Figure 1A). HH2 was designed to be an analog of HH16, a previously studied intermolecular configuration (Hertel et al., 1994; Hertel & Uhlenbeck, 1995) (Figure 1B). Both hammerheads yield the same 3′ cleavage product, P2, which does not dissociate at the RNA concentrations and temperatures used in these experiments. Sequence differences between the two hammerheads consist of a loop closing stem III of HH2 and a transition in stem III. These modifications do not alter the cleavage kinetics of the hammerheads (Long & Uhlenbeck, 1994).

The temperature dependence of the internal equilibrium measured for HH2 is shown in Figure 2. The standard free energy of the HH2 internal equilibrium, 2.2 kcal/mol at 298 K, agrees reasonably well with the 2.9 kcal/mol measured for HH16 (Hertel & Uhlenbeck, 1995). The entropies measured for the HH2 and HH16 internal equilibria (40 eu and 44 eu, respectively) are within experimental error, as are the enthalpies (9.6 kcal/mol for HH2 and 10 kcal/mol for HH16). Thus, the structural differences between these two hammerheads do not greatly affect their thermodynamic properties.

The dependence of the HH2 internal equilibrium on Mg^{2+} concentration is shown in Figure 3. Increasing Mg^{2+} concentration causes the internal equilibrium to shift toward uncleaved HH2, in agreement with the same experiment

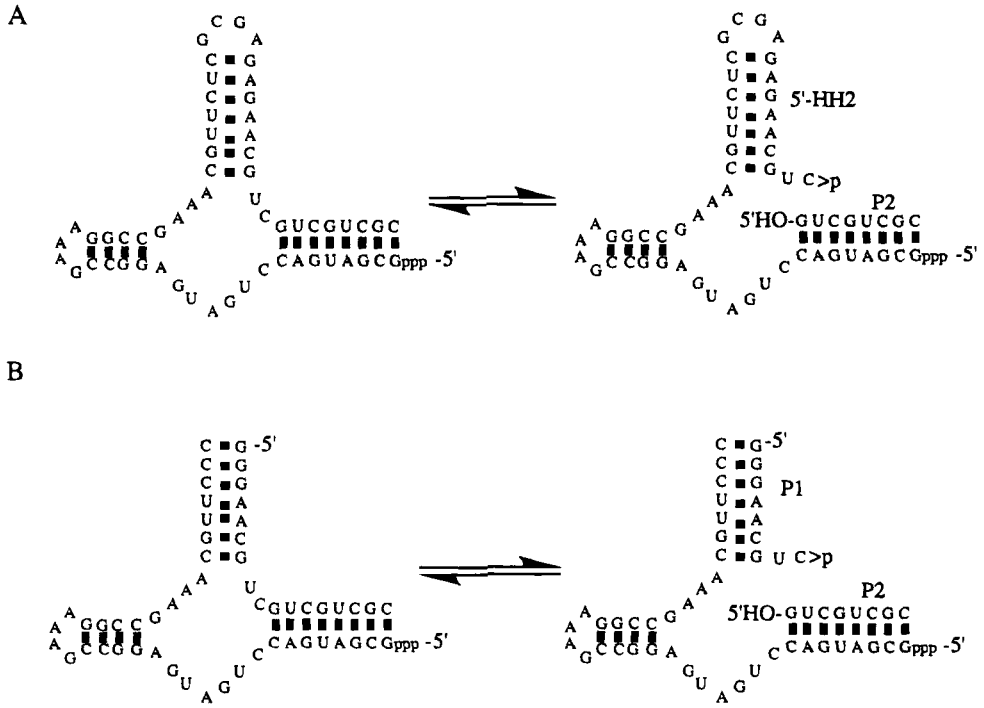

FIGURE 1: (A) Internal equilibrium of hammerhead 2 (HH2). The 5′ and 3′ cleavage products are 5′-HH2 and P2, respectively. (B) Internal equilibrium of hammerhead 16 (HH16). The 5′ and 3′ cleavage products are P1 and P2, respectively.

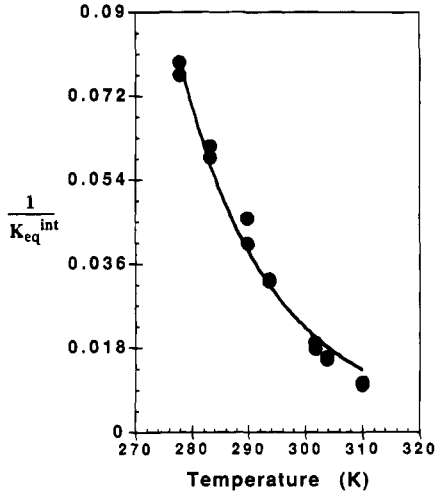

FIGURE 2: Temperature dependence of the HH2 internal equilibrium in 10 mM Mg^{2+} at pH 6.5. The solid line represents a theoretical fit to the equation $K_{eq}^{int} = \exp(-\Delta H/RT + \Delta S/R)$.

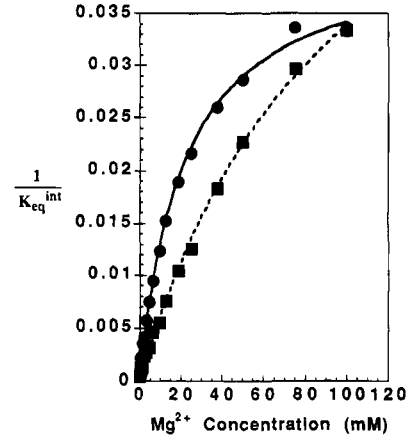

FIGURE 3: Internal equilibrium of HH2 at pH 6.5 as a function of Mg^{2-} concentration (●), and as a function of Mg^{2+} concentration with ionic strength held constant at 0.6 M with NaCl (■). The solid and dashed lines represent theoretical fits to the equation $1/K_{eq}^{int} = [M/(K_p + M)](1/K_{eq}^{sat})$ where M is the Mg^{2+} concentration, K_p is an apparent dissociation constant, and K_{eq}^{sat} is the internal equilibrium constant at saturating Mg^{2+} concentration.

performed with HH16 (Hertel & Uhlenbeck, 1995). The dependence of the internal equilibrium on Mg^{2+} concentration, which shows saturation at high Mg^{2+} concentration, has the hyperbolic form of a binding isotherm. To show that the Mg^{2+} dependence is not due to changes in ionic strength, the internal equilibrium was measured at constant ionic strength (μ = 0.6 M) by including NaCl in the buffer over a range of Mg^{2+} concentrations (Figure 3). The concentration at which Mg^{2+} causes half-saturation of the internal equilibrium was approximately 5-fold higher when NaCl was used to keep the ionic strength constant, indicating that Na^+ ions present in this experiment can compete with Mg^{2+}. However, in this experiment hyperbolic Mg^{2+} concentration dependence is also observed, showing that the phenomenon is not simply due to changes in ionic strength.

The internal equilibrium of HH2 was measured as a function of the concentrations of three additional divalent metal ions known to support catalysis (Dahm & Uhlenbeck, 1991; Dahm et al., 1993). In Figure 4A, the internal equilibria as a function of Co^{2+}, Mn^{2+}, Ca^{2+}, and Mg^{2+} concentration are compared. In all four cases, the internal equilibrium has a hyperbolic dependence on metal ion concentration. The data in Table 1 show that the value of the internal equilibrium constant at saturating metal ion concentrations varies only 2-fold for the four metal ions. However, the metal ion concentration at half-saturation of the internal equilibrium varies over a wider range (2.2 mM for Co^{2+} versus 32 mM for Ca^{2+}). Because the ionic strength is the same for a given concentration of all four metal ions, these results are additional evidence that the metal ion effect is not due to changing ionic strength. Figure 4B is a Hill plot of the metal ion internal equilibrium data (Hill, 1925). The linearity of these plots shows that the divalent metal ion effects are noncooperative for all four divalent metal ions over the concentration ranges shown.

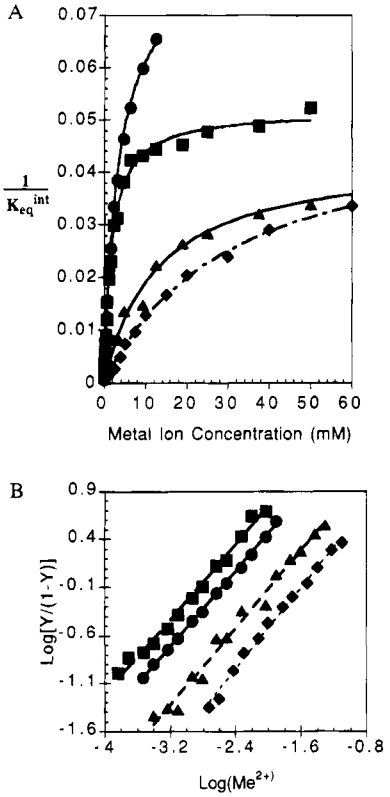

FIGURE 4: (A) Internal equilibrium of HH2 at pH 6.5 as a function of Ca^{2-} (♦), Co^{2+} (■), Mg^{2+} (▲), and Mn^{2-} (●) concentration. The lines represent theoretical fits to the equation $1/K_{eq}^{int} = [M/(K_p + M)](1/K_{eq}^{sat})$, where M is the metal ion concentration, K_p is an apparent dissociation constant, and K_{eq}^{sat} is the internal equilibrium constant at saturating metal ion concentration. (B) Hill plot for the internal equilibrium of HH2 in Ca^{2+} (♦), Co^{2+} (■), Mg^{2+} (▲), and Mn^{2+} (●). Y is the degree of saturation of the internal equilibrium ($Y = K_{eq}^{sat}/K_{eq}^{int}$). The slopes of the lines are 1.00 ± 0.05.

Table 1: Thermodynamic Parameters for the Metal Ion Dependence of the Hammerhead Internal Equilibrium

metal ion	K_p (mM)[a]	K_{eq}^{sat} [a]	K_{AMP} [b]
Ca^{2+}	32	19	12
Co^{2+}	2.2	19	2.4
Mg^{2+}	13	23	9.5
Mn^{2+}	4.0	12	3.5

[a] K_p and K_{eq}^{sat} values were obtained by fitting experimental data to the equation: $1/K_{eq}^{int} = [M/(K_p + M)](1/K_{eq}^{sat})$, where M is metal ion concentration, K_p is an apparent dissociation constant, and K_{eq}^{sat} is the internal equilibrium constant at saturating metal ion concentrations. [b] K_{AMP} values are dissociation constants for metal ion/5′AMP complexes (Smith et al., 1991).

Figure 5 shows the temperature dependencies of the internal equilibrium in the presence of 10 mM Mg^{2+}, Mn^{2+}, Ca^{2+}, and Co^{2+}. For all four metal ions, as temperature decreases the fraction of uncleaved RNA increases. However, the temperature dependencies for each metal are quantitatively different. At all temperatures, Mn^{2+} causes a higher fraction of uncleaved RNA than Co^{2+} and Mg^{2+}. At 277 K, 10 mM Mn^{2+} results in 23% ligated RNA, the highest observed extent of ligation.

Standard free energies, enthalpies, and entropies derived from the temperature dependence data are listed in Table 2. The equilibrium in the presence of all four divalent metal ions has a favorable positive entropy and unfavorable positive enthalpy. The 40 entropy units measured for the Co^{2+} and Mg^{2+} reactions are within experimental error as are the enthalpies of 10 and 9.6 kcal/mol for Co^{2+} and Mg^{2+},

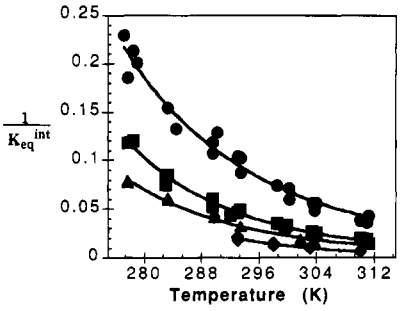

FIGURE 5: Temperature dependence of the HH2 internal equilibrium in 10 mM Ca^{2+} (♦), Co^{2+} (■), Mg^{2+} (▲), and Mn^{2+} (●) at pH 6.5. The solid lines represent theoretical fits to the equation $K_{eq}^{int} = \exp(-\Delta H/RT + \Delta S/R)$.

Table 2: Free Energies, Enthalpies, and Entropies of the Hammerhead Internal Equilibrium in 10 mM Metal Ions

metal ion (10 mM)	ΔG_{298} [b] (kcal/mol)	ΔH [a] (kcal/mol)	ΔS [a] (eu)
Ca^{2+}	−2.4	13	51
Co^{2+}	−1.9	10	40
Mg^{2+}	−2.3	9.6	40
Mn^{2+}	−1.5	8.3	33

[a] ΔH and ΔS values were obtained by fitting experimental data to the equation: $K_{eq}^{int} = \exp(-\Delta H/RT + \Delta S/R)$. [b] ΔG_{298} values were calculated from the relationship $\Delta G_{298} = \Delta H - T\Delta S$.

respectively. The relatively low favorable entropy of the Mn^{2+} reaction, 33 eu, is counteracted by a relatively low unfavorable enthalpy, 8.3 kcal/mol, while the relatively high favorable entropy of the Ca^{2+} reaction, 51 eu, is counteracted by a relatively high unfavorable enthalpy, 12.8 kcal/mol.

DISCUSSION

Although most studies address kinetic aspects of hammerhead catalysis, the chemistry and biology of this self-cleaving motif are dependent on thermodynamic properties as well. Because the internal equilibrium of the hammerhead reflects the relative stability of the cleaved and uncleaved RNAs, it is an important thermodynamic parameter. Only structural, dynamic, or other properties that distinguish the two RNAs, *and contribute differentially to the thermodynamic stability of each*, are detected in internal equilibrium measurements. Since the cleaved and uncleaved RNAs are similar in many respects, these measurements probe differences in thermodynamic stability that arise from relatively subtle changes in structure or dynamics. For example, the 2′,3′-cyclic phosphate present in the cleaved but not the uncleaved RNA must alter the relative stability of the two RNAs, but stems I, II, and III to lesser extent because they probably exist in both forms of the hammerhead. Similarly, only external variables that affect the stability of the two RNAs differentially, for example, temperature and metal ion concentration, are reflected in the internal equilibrium.

A particular advantage of hammerhead internal equilibrium measurements is that they are considerably more reproducible than kinetic measurements. This is primarily because the ratio of cleaved to uncleaved RNA is independent of time as long as the incubation period is sufficient to have reached equilibrium. The high precision of internal equilibrium measurements results in changes as small as 20% being significant.

Using a new method, we measured K_{eq}^{int} for HH2 and compared the results with those obtained using the previously reported method for HH16 (Hertel & Uhlenbeck, 1995). The

two hammerheads, one of which is intramolecular (HH2) and the other intermolecular (HH16), have similar K_{eq}^{int}s over a wide range of experimental conditions. The small observed differences in K_{eq}^{int} are attributable to the experimental methods used to characterize each. The method used to measure K_{eq}^{int} of HH16 requires that P1 and P2 be preannealed to the ribozyme, while the method used to characterize HH2 requires only P2 to be preannealed because P1 is covalently attached to the ribozyme *via* loop III. Thus, aberrant hybridization of P1 in the HH16 protocol could account for the lower extent of ligation observed for this hammerhead.

Taken together with the earlier observation that cleavage kinetics for HH2 are similar to those measured for HH16 (Long & Uhlenbeck, 1994), the similar K_{eq}^{int}s of the two shows that the free energy profiles for reactions catalyzed by intramolecular and intermolecular hammerheads can be similar. This is significant because natural hammerheads are believed to be intramolecular, but most studies of hammerhead catalysis have employed intermolecular hammerheads.

Given that hammerhead catalysis is dependent on metal ions interacting with the uncleaved hammerhead, and that the cleaved hammerhead, like all RNAs, must interact with metal ions as well, it is reasonable to propose Scheme 1 as a general description of how metal ion concentrations might affect the internal equilibrium.

Scheme 1

$$S + M \overset{K_s}{\rightleftharpoons} S{\cdot}M \overset{K_{eq}^{sat}}{\rightleftharpoons} P{\cdot}M \overset{K_p}{\rightleftharpoons} P + M$$

M represents metal ions, S is the uncleaved RNA, P is the cleaved RNA, S·M is a metal ion complex with S, P·M is a metal ion complex with P, K_s is an apparent dissociation constant for S·M, K_p is an apparent dissociation constant for P·M, and K_{eq}^{sat} is the equilibrium ratio between S·M and P·M, and is equal to K_{eq}^{int} at fully saturating metal ion concentrations. The stoichiometries of S·M and P·M have not been specified to make the model generally applicable, and it applies to cooperative as well as noncooperative metal ion binding.

The gel methods used to measure the internal equilibrium cannot distinguish the free RNAs from the metal ion complexes. Thus, the measured ratio of uncleaved to cleaved RNA ($1/K_{eq}^{int}$) includes the free RNAs as well as the metal ion complexes. Equation 1, which gives $1/K_{eq}^{int}$ as a function of metal ion concentration, is derived from Scheme 1.

$$\frac{S + S{\cdot}M}{P + P{\cdot}M} = \frac{1}{K_{eq}^{int}} = \frac{1}{K_{eq}^{sat}}\left(\frac{K_s + M}{K_p + M}\right) \quad (1)$$

Equation 1 shows that the internal equilibrium will be independent of metal ion concentration if K_s and K_p are equal. If K_p is larger than K_s however, the internal equilibrium will shift toward ligated RNA as the metal ion concentration is increased. This is the observed effect (Figure 3), and is easily distinguishable from the case where K_s is larger than K_p, which would give the reciprocal metal ion dependence. The observed hyperbolic dependence, where $1/K_{eq}^{int}$ extrapolates to zero at low metal ion concentration, is consistent with a noncooperative binding isotherm. From the *y*-intercept of the metal ion concentration curves (Figure 3) and eq 1, we estimate the upper limit for K_s at one-fifth K_p. Equation 1 approximates a binding equation (eq 2) when K_s is much smaller than M.

$$\frac{S + S{\cdot}M}{P + P{\cdot}M} = \frac{1}{K_{eq}^{int}} = \frac{1}{K_{eq}^{sat}}\left(\frac{M}{K_p + M}\right) \quad (2)$$

Thus, in terms of Scheme 1, the shift toward ligated RNA as metal ion concentration is increased results from metal ion dissociation from the cleaved RNA. It follows that the metal ion concentration at which the internal equilibrium is half-saturated is a measure of K_p, and that at saturating metal ion concentrations the internal equilibrium is equal to $1/K_{eq}^{sat}$. K_{eq}^{sat} and K_p values listed in Table 1 for different metal ions are derived from eq 2 and the experimental data shown in Figure 4A.

If the metal ion dependence of the internal equilibrium is the result of metal ion dissociation from the cleaved hammerhead, then it is informative to compare the K_ps with dissociation constants measured for other RNA/metal ion complexes. The best studied examples of metal ion binding to RNA are tRNA with various metal ions (Danchin, 1972; Schreier & Schimmel, 1974; Jack et al., 1977). tRNA has two classes of metal ion binding sites: "strong" sites which are site-specific and "weak" sites which are nonspecific. The K_ps for Co^{2+}, Mn^{2+}, and Mg^{2+} are similar to the Kds measured for nonspecific binding to tRNA and approximately 100-fold weaker than site-specific binding to tRNA. Also, the observed order and absolute values of the K_ps correlate with dissociation constants measured for metal ions complexed with 5′AMP (K_{AMP}) (Table 1). Because 5′AMP and the hammerhead RNA both have phosphate oxygens and N7 of adenine, which are potential metal ion ligands, we postulate that this correlation could arise from metal ion dissociation from a hammerhead binding site containing N7 of a purine residue and a phosphate oxygen atom. Indeed, a metal ion binding site containing N7 of a guanine residue and a phosphate oxygen atom has been identified in the crystal structure of a hammerhead ribozyme/inhibitor complex (Pley et al., 1994).

The internal equilibrium at saturating concentrations of Ca^{2+}, Co^{2+}, Mn^{2+}, and Mg^{2+} is reflected by different K_{eq}^{sat} values listed in Table 1. Because the free energy of the internal equilibrium under these conditions is independent of metal ion concentration, K_{eq}^{sat} does not contain, per se, information about intermolecular RNA/metal ion interactions. Rather, it is a measure of the relative thermodynamic stability of the RNA/metal ion complexes S·M and P·M. Since S·M and P·M must be similar in many respects, the comparative nature of K_{eq}^{sat} makes it a particularly useful quantity. Since the metal ions have different ligand coordination properties (Sigel, 1993; Sigel et al., 1994), changes in K_{eq}^{sat} could be the result of altered structure between the S·M and P·M complexes. This altered structure could be as subtle as changes in metal ion/RNA bond distances and energies, or perhaps as conspicuous as changes in the identity of ligands or the number of bound metal ions. In this last regard, different K_{eq}^{sat} values and saturation behaviors of the internal equilibrium do not reveal how many metal ions are bound to the RNAs under saturating conditions. Because the Hill coefficients for all the metal ions are unity (Figure 4B), either dissociation from P·M involves only one metal ion or multiple ions dissociate in a noncooperative manner. The data are not consistent with cooperative metal ion dissociation from P·M.

It is not justifiable, on the basis of this correlation alone, to conclude that the metal ion dependence of the hammerhead internal equilibrium derives from nonspecific metal ion binding. Indeed, site specifically bound metal ions are clearly identifiable in two recently solved X-ray crystal structures of hammerhead ribozyme/inhibitor complexes (Pley et al., 1994; Scott et al., 1995). Although these metal ions are not necessarily the ones that play important roles in the internal equilibrium or other solution properties of the hammerhead, the internal equilibrium studies presented here provide a basis for addressing this issue. By employing RNAs with chemically modified nucleotides, which based on the crystal structure are predicted to have altered metal ion ligands (and thus different metal ion affinities), internal equilibrium experiments might show if metal ion binding is site-specific and where on the RNAs the metal ions bind.

The temperature dependence of the internal equilibrium was measured at 10 mM metal ion, which is subsaturating to different extents for each ion. We were unable to collect data for Ca^{2+} reactions at low temperatures because degradation of the hammerhead occurred before equilibrium was reached. Entropy and enthalpy changes for the internal equilibrium were calculated from the temperature dependence data and are reported in Table 2. Consequently, the values contain different contributions from both the metal ion dependent fraction (K_p) and the metal ion independent fraction (K_{eq}^{sat}) of the total free energy. One conclusion that can be drawn from the data in Table 2 is that ΔH is metal ion dependent, and therefore does not simply reflect the formation of 2′,3′-cyclic phosphate as was originally hypothesized (Hertel & Uhlenbeck, 1995). Based on the measured variation in ΔS and ΔH for metal ion binding to nucleotides, which contain the same ligands characteristic of RNA, it is perhaps not surprising that the thermodynamics of the internal equilibrium are different in the presence of each ion (Smith et al., 1991). Nonetheless, the large magnitudes and absolute values of ΔS and ΔH for the internal equilibrium in the presence of all the ions studied indicate that the RNA itself makes large contributions to these thermodynamics. By measuring the internal equilibrium as a function of temperature at different metal ion concentrations, we intend to deconvolute contributions made by the metal ions and the RNA.

How important is the metal ion concentration dependent fraction of the internal equilibrium free energy? By comparing the internal equilibrium at saturating metal ion concentration with that at 10 mM Mg^{2+}, a standard condition for in vitro hammerhead studies, it can be shown 20% of the free energy is a result of metal ion dissociation under the latter condition. The contribution to the free energy that metal ion dissociation is expected to make at the lower metal ion concentrations found in vivo would be much larger. However, equilibria estimated from in vivo ratios of cleaved and uncleaved viroid RNAs containing hammerheads appear to be different from the in vitro measurements presented here. Indeed, greater than 90% of avocado sun blotch viroid RNA isolated from plant cells is circular (ligated), indicating that the in vivo K_{eq}^{int} of this viroid could be as much as 50-fold lower than predicted from our in vitro measurements (Keese & Symons, 1987). This difference is too large to be explained in terms of metal ion concentration or other variables that affect the internal equilibrium in vitro. It can be, however, explained in terms of accumulation of circular viroid RNA that cannot cleave. Such inactive conformations might be, for example, the rod-shaped secondary structures proposed for circular viroids that do not have the hammerhead secondary structure (Keese & Symons, 1987; Miller & Silver, 1991). Consequently, thermodynamic properties of the hammerhead motif itself might be important in biological processes, namely, viroid replication, but these are probably context-dependent and modulated by properties of the RNAs in which they are embedded.

ACKNOWLEDGMENT

We thank Tracy K. Stage and Doug Turner for critical reading of the manuscript.

REFERENCES

Dahm, S. C., & Uhlenbeck, O. C. (1991) *Biochemistry 30,* 9464−9469.
Dahm, S. C., Derrick, W. B., & Uhlenbeck, O. C. (1993) *Biochemistry 32,* 13040−13045.
Danchin, A. (1972) *Biopolymers 11,* 1317−1333.
Fedor, M. J., & Uhlenbeck, O. C. (1990) *Proc. Natl. Acad. Sci. U.S.A. 87,* 1668−1672.
Fedor, M. J., & Uhlenbeck, O. C. (1992) *Biochemistry 31,* 12042−12054.
Haseloff, J., & Gerlach, W. L. (1988) *Nature 334,* 585−591.
Hertel, K. J., & Uhlenbeck, O. C. (1995) *Biochemistry 34,* 1744−1749.
Hertel, K. J., Hershlag, D., & Uhlenbeck, O. C. (1994) *Biochemistry 33,* 3374−3385.
Hill, R. (1925) *Proc. Res. Soc. B100,* 419.
Jack, A., Ladner, D. R., Brown, R. S., & Klug, A. (1977) *J. Mol. Biol. 111,* 315−328.
Keese, P., & Symons, R. H. (1987) in *Viroids and Viroid-Like Pathogens* (Semancik, J. S., Ed.) pp 1−47, CRC Press Inc., Boca Raton, FL.
Long, D. M., & Uhlenbeck, O. C. (1993) *FASEB J. 7,* 25−30.
Long, D. M., & Uhlenbeck, O. C. (1994) *Proc. Natl. Acad. Sci. U.S.A. 91,* 6977−6981.
Miller, W. A., & Silver, S. L. (1991) *Nucleic Acids Res. 19,* 5313−5320.
Milligan, J. F., & Uhlenbeck, O. C. (1989) *Methods Enzymol. 180,* 51−62.
Pley, H. W., Flaherty, K. M., & McKay, D. B. (1994) *Nature 372,* 68−74.
Prody, G. A., Bakos, J. T., Buzayan, J. M., Schneider, I. R., & Bruening, G. (1986) *Science 231,* 1577−1580.
Schreier, A. A., & Schimmel, P. R. (1974) *J. Mol. Biol. 86,* 601−620.
Scott, W., Finch, J., & Klug, A. (1995) *Cell 81,* 991−1002.
Sigel, H. (1993) *Reviews 22,* 255.
Sigel, H., Massoud, S. S., & Corfu, N. A. (1994) *J. Am. Chem. Soc. 116,* 2958−2971.
Slim, G., & Gait, M. J. (1991) *Nucleic Acids Res. 19,* 1183−1188.
Smith, R. M., Martell, A. E., & Chen, Y. (1991) *Pure Appl. Chem. 63,* 1015−1080.
Symons, R. H. (1992) *Annu. Rev. Biochem. 61,* 641−671.
Uhlenbeck, O. C. (1987) *Nature 328,* 596−600.
Williams, D. M., Pieken, W. A., & Eckstein, F. (1992) *Proc. Natl. Acad. Sci. U.S.A. 89,* 918−921.

BI951552A